International Journal of Heat and Mass Transfer 52 (2009) 2300–2310

Contents lists available at ScienceDirect

International Journal of Heat and Mass Transfer

journal homepage: www.elsevier.com/locate/ijhmt

Stability analysis of dual adiabatic flows in a horizontal porous layer

A. Barletta [a,*], D.A.S. Rees [b]

[a] Dipartimento di Ingegneria Energetica, Nucleare e del Controllo Ambientale (DIENCA), Università di Bologna, Via dei Colli 16, I-40136 Bologna, Italy
[b] Department of Mechanical Engineering, University of Bath, Bath BA2 7AY, UK

ARTICLE INFO

Article history:
Received 30 May 2008
Available online 18 January 2009

Keywords:
Laminar flow
Mixed convection
Darcy model
Porous medium
Linear stability
Viscous dissipation

ABSTRACT

A study of buoyant flow in a horizontal porous layer with adiabatic and impermeable boundaries is performed. The Darcy–Boussinesq model is used and the effect of viscous dissipation is taken into account. First, it is shown that there exist two stationary and parallel solutions (*dual solutions*) for each pair of prescribed values of the Gebhart number *Ge* and of the Péclet number *Pe*. These dual solutions exist as long as $Ge \leqslant \sqrt{3}$, and they become coincident when $Ge = \sqrt{3}$. Then, a linear stability analysis of the dual solutions is performed referring both to transverse and to longitudinal rolls. This analysis reveals that one of the branches in the dual solutions space is more stable than the other. Moreover, instabilities to longitudinal rolls generally occur for values of the product *GePe* smaller than those needed for transverse rolls.

1. Introduction

As is well known, the effect of viscous dissipation may be important especially under conditions of very small boundary heat fluxes and, in particular, when the flow system is bounded by thermally insulating surfaces [1]. Also the fluid properties, the size of the channel or duct and the flow regime may contribute to enhance the effect of viscous dissipation. In fact, this effect becomes important when the fluid has a relatively small thermal conductivity or a high viscosity, or when the mass flow rate is sufficiently high. Viscous dissipation may be considerable when the fluid flow is constrained within passages of very small size as the microchannels [2] or in the case of flows in fluid-saturated porous media [3,4]. As it has been pointed out in several papers [5–9], the effect of viscous dissipation may contribute, under certain conditions, to the build up of temperature gradients that are capable of inducing buoyancy effects on the flow. These effects may be rather significant so that, in some flow arrangements, the origin of convective roll instabilities is the vertical thermal gradient induced by viscous dissipation and not, as usually happens, the temperature differences due to the boundary conditions. From a mathematical viewpoint, the cause of these instabilities is the nonlinear viscous dissipation term appearing in the local energy balance equation. Moreover, the nonlinear nature of the viscous dissipation term may also influence the features of the basic flows upon which the disturbances are superimposed. In fact, it has been shown that the viscous dissipation can lead to dual solutions for stationary buoyant flows [10,11].

The onset of convective instabilities in fluid-saturated porous media is a subject widely treated in the literature of the last decades. Reviews of the main results obtained in this field are available in Refs. [12–14]. A widely analysed kind of instability is the well-known Horton–Rogers–Lapwood problem (HRL) [15,16], also known as the Darcy–Bénard problem. The HRL problem is the porous-medium analogue of the usual Rayleigh–Bénard problem for clear fluids. One considers an infinite horizontal porous layer such that its bottom boundary is subject to a uniform temperature higher than that prescribed on the top boundary. A sufficiently high temperature difference between the boundaries, *i.e.* a sufficiently high Darcy–Rayleigh number, leads to the onset of rolls instabilities. In particular, it is well known that the critical value of the Darcy–Rayleigh number for the formation of convective rolls in an unbounded layer is $4\pi^2$ [12–14]. An important variant of the HRL problem is the Prats problem [17]. In the Prats problem, the basic solution is a uniform horizontal flow instead of a rest state. The horizontal flow does not affect either the critical value of the Darcy–Rayleigh number nor the critical wave number of the rolls disturbance, as the stability analysis may be referred to an inertial reference frame comoving with respect to the basic flow. The effects of the inertial term in the momentum equation have been analysed by He and Georgiadis [18] and by Rees [19].

A few papers have investigated the effect of viscous dissipation with respect to the onset of convective instabilities [6,20,21]. Mureithi and Mason [6] develop a study of convective linear instabilities for a boundary layer flow with an accelerating free-stream profile. They show that viscous dissipation may cause the existence

* Corresponding author.
E-mail addresses: antonio.barletta@mail.ing.unibo.it (A. Barletta), d.a.s.rees@bath.ac.uk (D.A.S. Rees).

0017-9310/$ - see front matter © 2008 Elsevier Ltd. All rights reserved.
doi:10.1016/j.ijheatmasstransfer.2008.12.002

Nomenclature

a	nondimensional wave number, Eqs. (39) and (55)
A_n	nth series coefficient, Eq. (A1)
c	nondimensional speed of the transverse rolls, Eq. (49)
c_p	specific heat at constant pressure
g	modulus of gravitational acceleration
$\mathbf{g}$	gravitational acceleration
Ge	Gebhart number, Eq. (13)
K	permeability
L	channel height
n	integer number
Pe	Péclet number, Eq. (18)
R	nondimensional parameter, Eq. (47)
$\Re$	real part
t	nondimensional time, Eq. (7)
T	nondimensional temperature, Eq. (7)
$\hat{T}$	nondimensional function, Eq. (15)
$\tilde{T}_{B\pm}$	nondimensional functions, Eq. (21)
u, v, w	nondimensional velocity components, Eq. (7)
U, V, W	nondimensional velocity disturbances, Eq. (28)
$\bar{u}_{Bm}$	average horizontal velocity of the base flow
$\tilde{u}_{B\pm}$	nondimensional functions, Eq. (21)
x, y, z	nondimensional coordinates, Eq. (7)

Greek symbols

α	thermal diffusivity
β	volumetric coefficient of thermal expansion
γ	reduced exponential coefficient, Eq. (47)
ε	nondimensional perturbation parameter, Eq. (28)
Γ	nondimensional constant, Eq. (15)
$\Gamma_\pm$	nondimensional constants, Eqs. (19) and (20)
$\tilde{\Gamma}_\pm$	nondimensional constants, Eq. (21)
θ	nondimensional temperature disturbance, Eq. (28)
$\Theta(y)$	nondimensional function, Eqs. (39) and (55)
λ	exponential coefficient, Eqs. (39) and (55)
λ_1, λ_2	real and imaginary parts of λ
ν	kinematic viscosity
ρ	mass density
σ	heat capacity ratio
$\Phi(y)$	nondimensional function such that $\Psi(y) = iaGe\Phi(y)$
ψ	nondimensional streamfunction, Eqs. (35) and (51)
$\Psi(y)$	nondimensional function, Eqs. (39) and (55)

Superscripts, subscripts

$\bar{}$	dimensional quantity
B	base flow
cr	critical value

of three unstable modes, while one single inviscid unstable mode exists in the limit of negligible viscous dissipation. Rees et al. [20] investigate the onset of transverse rolls instability in the asymptotic dissipation profile (ADP), *i.e.* a parallel external flow solution for the boundary layer around an inclined cold surface embedded in a porous medium. These authors show that the ADP is stable as long as the cold surface is vertical; when the surface is inclined, the critical Darcy–Rayleigh number is a decreasing function of the inclination angle with respect to the vertical direction. In a recent paper [21], the onset of convective instabilities in a horizontal porous layer with adiabatic bottom boundary and perfectly or imperfectly isothermal top boundary is investigated. The basic solution considered in Ref. [21] is the unique stationary, parallel, horizontal flow solution: a uniform velocity profile with a purely vertical, linearly varying temperature gradient. In the basic solution, the temperature gradient is built up as a consequence of the viscous heating in the porous medium.

The aim of the present paper is the study of the linear stability against transverse and longitudinal rolls of the viscous-heating buoyant flow in a horizontal porous layer. The boundary planes of the porous layer are assumed to be adiabatic and impermeable, so that viscous dissipation is the only thermal effect occurring in the flow system. First, it is shown that the basic steady flow compatible with the assumption of parallel velocity field is not uniquely defined, as the governing equations admit dual solutions for assigned mass flow rate, fluid/solid properties and layer thickness. Then, the stability of these basic dual flows is studied with respect to transverse and longitudinal rolls disturbances.

2. Governing equations

Let us consider laminar flow in an infinitely wide and horizontal fluid-saturated porous layer with height L (see Fig. 1). The Darcy–Boussinesq model is adopted to include the effect of buoyancy. The components of seepage velocity along the $\bar{x}$-direction, $\bar{y}$-direction and $\bar{z}$-direction are denoted by $\bar{u}$, $\bar{v}$ and $\bar{w}$, respectively. Temperature is denoted by $\bar{T}$ and time by $\bar{t}$. Both the boundary walls, $\bar{y} = 0, L$, are assumed to be perfectly insulated and impermeable.

The governing mass, momentum and energy balance equations can be expressed as

$$\frac{\partial \bar{u}}{\partial \bar{x}} + \frac{\partial \bar{v}}{\partial \bar{y}} + \frac{\partial \bar{w}}{\partial \bar{z}} = 0, \tag{1}$$

$$\frac{\partial \bar{w}}{\partial \bar{y}} - \frac{\partial \bar{v}}{\partial \bar{z}} = -\frac{g\beta K}{\nu}\frac{\partial \bar{T}}{\partial \bar{z}}, \tag{2}$$

$$\frac{\partial \bar{u}}{\partial \bar{z}} - \frac{\partial \bar{w}}{\partial \bar{x}} = 0, \tag{3}$$

$$\frac{\partial \bar{v}}{\partial \bar{x}} - \frac{\partial \bar{u}}{\partial \bar{y}} = \frac{g\beta K}{\nu}\frac{\partial \bar{T}}{\partial \bar{x}}, \tag{4}$$

$$\sigma\frac{\partial \bar{T}}{\partial \bar{t}} + \bar{u}\frac{\partial \bar{T}}{\partial \bar{x}} + \bar{v}\frac{\partial \bar{T}}{\partial \bar{y}} + \bar{w}\frac{\partial \bar{T}}{\partial \bar{z}} = \alpha\left(\frac{\partial^2 \bar{T}}{\partial \bar{x}^2} + \frac{\partial^2 \bar{T}}{\partial \bar{y}^2} + \frac{\partial^2 \bar{T}}{\partial \bar{z}^2}\right) + \frac{\nu}{Kc_p}\left(\bar{u}^2 + \bar{v}^2 + \bar{w}^2\right), \tag{5}$$

where σ is the ratio between the average volumetric heat capacity $(\rho c_p)_m$ of the porous medium and the volumetric heat capacity $(\rho c_p)_f$ of the fluid, g is the modulus of the gravitational acceleration g, β is the volumetric coefficient of thermal expansion, K is the permeability, ν is the kinematic viscosity, α is the thermal diffusivity and c_p is the specific heat at constant pressure. Eqs. (2)–(4) have been obtained by applying the curl operator to both sides of the Darcy momentum balance equation in order to remove the explicit dependence on the pressure field.

Velocity and temperature boundary conditions are expressed as

$$\bar{y} = 0, L: \quad \bar{v} = 0 = \frac{\partial \bar{T}}{\partial \bar{y}}. \tag{6}$$

2.1. Dimensionless equations

Let us introduce dimensionless variables such that

$$(\bar{x}, \bar{y}, \bar{z}) = (x, y, z)L, \quad \bar{t} = t\frac{\sigma L^2}{\alpha}, \quad (\bar{u}, \bar{v}, \bar{w}) = (u, v, w)\frac{\alpha}{L}, \quad \bar{T} = T\frac{\nu\alpha}{Kc_p}. \tag{7}$$

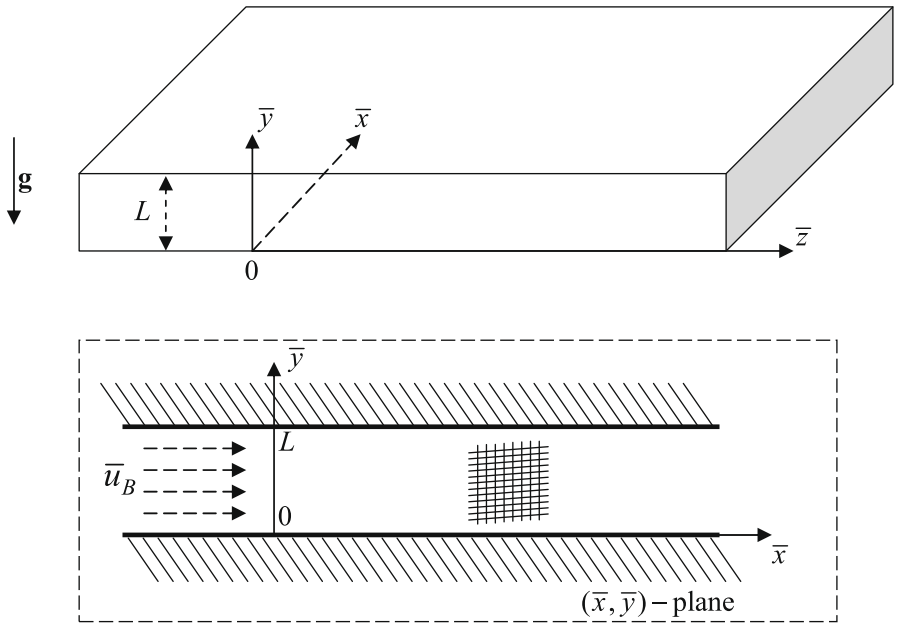

Fig. 1. Sketch of the porous layer.

Then, Eqs. (1)–(5) can be rewritten as

$$\frac{\partial u}{\partial x}+\frac{\partial v}{\partial y}+\frac{\partial w}{\partial z}=0, \tag{8}$$

$$\frac{\partial w}{\partial y}-\frac{\partial v}{\partial z}=-Ge\frac{\partial T}{\partial z}, \tag{9}$$

$$\frac{\partial u}{\partial z}-\frac{\partial w}{\partial x}=0, \tag{10}$$

$$\frac{\partial v}{\partial x}-\frac{\partial u}{\partial y}=Ge\frac{\partial T}{\partial x}, \tag{11}$$

$$\frac{\partial T}{\partial t}+u\frac{\partial T}{\partial x}+v\frac{\partial T}{\partial y}+w\frac{\partial T}{\partial z}=\frac{\partial^2 T}{\partial x^2}+\frac{\partial^2 T}{\partial y^2}+\frac{\partial^2 T}{\partial z^2}+u^2+v^2+w^2, \tag{12}$$

where the Gebhart number, given by,

$$Ge=\frac{g\beta L}{c_p}, \tag{13}$$

has been used. The boundary conditions (6) may be expressed in a dimensionless form as

$$y=0,1: \quad v=0=\frac{\partial T}{\partial y}. \tag{14}$$

2.2. Dual base flows

Under the assumptions of steady parallel flow with a constant temperature gradient in the $\bar{x}$-direction, *i.e.*

$$v=0=w, \quad T=\Gamma x+\hat{T}(y), \tag{15}$$

where Γ is a constant, Eqs. (8)–(12) are simplified greatly. In fact, one obtains

$$\frac{\partial u}{\partial x}=0, \quad \frac{\partial u}{\partial z}=0, \quad \frac{\partial u}{\partial y}=-\Gamma Ge, \quad \frac{d^2\hat{T}}{dy^2}-\Gamma u+u^2=0. \tag{16}$$

The base flow solution is easily obtained from Eqs. (15) and (16) and from the boundary conditions Eq. (14),

$$\begin{aligned} u_B &= Pe-\frac{\Gamma Ge}{2}(2y-1), \quad v_B=0=w_B,\\ \hat{T}_B &= -\frac{1}{12}Ge^2\Gamma^2y^4+\frac{Ge\Gamma}{6}(Ge\Gamma-\Gamma+2Pe)y^3\\ &\quad -\frac{1}{8}\left(4Pe^2+4Ge\Gamma Pe-4\Gamma Pe+Ge^2\Gamma^2-2Ge\Gamma^2\right)y^2, \end{aligned} \tag{17}$$

where

$$Pe=\frac{\bar{u}_{Bm}L}{\alpha} \tag{18}$$

is the Péclet number based on the average horizontal velocity $\bar{u}_{Bm}$. Moreover, since in Eqs. (8)–(12) and (14) the temperature field is defined only up to an arbitrary additive constant, in Eq. (17) this constant has been fixed so that $\hat{T}_B(0)=0$.

In order to fulfil the boundary conditions Eq. (14), the three parameters (Ge,Γ,Pe) are not independent. If one fixes any pair among these three parameters, the third parameter admits two different determinations. For instance, if one assumes that Ge and Pe are assigned, then Γ can be given either by

$$\Gamma=\Gamma_+=\frac{6Pe}{Ge^2}\left(1+\sqrt{1-\frac{Ge^2}{3}}\right), \tag{19}$$

or by

$$\Gamma=\Gamma_-=\frac{6Pe}{Ge^2}\left(1-\sqrt{1-\frac{Ge^2}{3}}\right). \tag{20}$$

It is easily verified that Eqs. (17), (19) and (20) define dual parallel base flows such that

$$\begin{aligned} &Ge,\Gamma_\pm,Pe)=Pe\tilde{u}_{B\pm}(y;Ge),\\ &\hat{T}_B(y;Ge,\Gamma_\pm,Pe)=Pe^2\tilde{T}_{B\pm}(y;Ge), \quad \Gamma_\pm(Ge,Pe)=Pe\tilde{\Gamma}_\pm(Ge), \end{aligned} \tag{21}$$

where functions u_B and $\hat{T}_B$ are those obtained through Eq. (17). There are three important features of the dual solutions given in Eq. (21):

- positive values of Ge and Pe yield real positive values of both Γ_- and Γ_+, provided that $Ge\leqslant\sqrt{3}$;

- dual solutions are distinct for $Ge < \sqrt{3}$, while they coincide for $Ge = \sqrt{3}$;
- no parallel base flow solutions are allowed if $Ge > \sqrt{3}$.

Note that, for given Pe and Ge, $\tilde{u}_{B+}$ and $\tilde{u}_{B-}$ share the same average value, while they differ merely by the slope of the linear change along y.

It must be pointed out that, in the limit $Ge \to 0$, functions $\tilde{u}_{B+}(y;Ge)$, $\tilde{T}_{B+}(y;Ge)$ and $\tilde{\Gamma}_{+}(Ge)$ are singular,

$$\tilde{u}_{B+}(y;Ge) = -\frac{6(2y-1)}{Ge} + 1 + O(Ge), \tag{22}$$

$$\tilde{T}_{B+}(y;Ge) = -\frac{12y^2(2y-3)}{Ge^3} - \frac{12y^2(y-1)^2}{Ge^2} + O\left(Ge^{-1}\right), \tag{23}$$

$$\tilde{\Gamma}_{+}(Ge) = \frac{12}{Ge^2} - 1 - \frac{Ge^2}{12} + O\left(Ge^4\right), \tag{24}$$

while $\tilde{u}_{B-}(y;Ge)$, $\tilde{T}_{B-}(y;Ge)$ and $\tilde{\Gamma}_{-}(Ge)$ are regular,

$$\tilde{u}_{B-}(y;Ge) = 1 - \frac{1}{2}(2y-1)Ge - \frac{1}{24}(2y-1)Ge^3 + O\left(Ge^5\right), \tag{25}$$

$$\tilde{T}_{B-}(y;Ge) = \frac{1}{12}y^2(2y-3)Ge - \frac{1}{12}y^2(y-1)^2Ge^2 + O\left(Ge^4\right), \tag{26}$$

$$\tilde{\Gamma}_{-}(Ge) = 1 + \frac{Ge^2}{12} + \frac{Ge^4}{72} + O\left(Ge^6\right). \tag{27}$$

The limit $Ge \to 0$, physically, represents the forced convection regime where buoyancy does not affect fluid flow. In this limit, only the solution branch $\{\tilde{u}_{B-}, \tilde{T}_{B-}\}$ is meaningful and, on account of Eqs. (15), (21), (25)–(27), one has a uniform flow with $u_B = Pe$ and $T_B = Pex$.

Fig. 2 displays the behaviour of the profiles $\tilde{T}_{B-}$ and $\tilde{T}_{B+}$ for different values of Ge. An important feature of the plots reported in Fig. 2 is that both $\tilde{T}_{B-}(y)$ and $\tilde{T}_{B+}(y)$ are monotonic functions for $Ge \leqslant 3/2$. In this range, $\tilde{T}_{B-}$ is a decreasing function of y, while $\tilde{T}_{B+}$ is an increasing function of y. A physical consequence of this behaviour is that, for $Ge \leqslant 3/2$, the solution branch $\{\tilde{u}_{B+}, \tilde{T}_{B+}\}$ would not develop convective instabilities, since the vertical temperature gradient of the base flow is opposed to gravity. With a similar reasoning, one may infer that the solution branch $\{\tilde{u}_{B-}, \tilde{T}_{B-}\}$ may develop convective instabilities for any value of Ge in the range $0 < Ge \leqslant \sqrt{3}$.

2.3. Linearisation

Disturbances (U, V, W, θ) of the base flow given by Eqs. (15), (17) and (21) are defined as

$$\begin{aligned} u &= Pe\tilde{u}_{B\pm} + \varepsilon U, \quad v = \varepsilon V, \quad w = \varepsilon W, \\ T &= Pe\tilde{\Gamma}_{\pm}x + Pe^2\tilde{T}_{B\pm} + \varepsilon\theta, \end{aligned} \tag{28}$$

where ε is a very small perturbation parameter. On substituting Eq. (28) in Eqs. (8)–(12) and neglecting nonlinear terms in the perturbations, *i.e.* terms of order ε^2, one obtains

$$\frac{\partial U}{\partial x} + \frac{\partial V}{\partial y} + \frac{\partial W}{\partial z} = 0, \tag{29}$$

$$\frac{\partial W}{\partial y} - \frac{\partial V}{\partial z} = -Ge\frac{\partial \theta}{\partial z}, \tag{30}$$

$$\frac{\partial U}{\partial z} - \frac{\partial W}{\partial x} = 0, \tag{31}$$

$$\frac{\partial V}{\partial x} - \frac{\partial U}{\partial y} = Ge\frac{\partial \theta}{\partial x}, \tag{32}$$

$$\frac{\partial \theta}{\partial t} + Pe\tilde{u}_{B\pm}\frac{\partial \theta}{\partial x} + Pe^2V\frac{d\tilde{T}_{B\pm}}{dy} = \frac{\partial^2\theta}{\partial x^2} + \frac{\partial^2\theta}{\partial y^2} + \frac{\partial^2\theta}{\partial z^2} + Pe\left(2\tilde{u}_{B\pm} - \tilde{\Gamma}_{\pm}\right)U. \tag{33}$$

3. Instability with respect to transverse rolls

Let us consider disturbances for rolls which are parallel to the $\bar{z}$-direction, namely

$$U = U(x,y,t), \quad V = V(x,y,t), \quad W = 0, \quad \theta = \theta(x,y,t). \tag{34}$$

Then, on introducing a streamfunction ψ, such that

$$U = \frac{\partial \psi}{\partial y}, \quad V = -\frac{\partial \psi}{\partial x}, \tag{35}$$

Eqs. (29)–(31) are identically satisfied, while Eqs. (32) and (33) may be rewritten in the form

$$\frac{\partial^2\psi}{\partial x^2} + \frac{\partial^2\psi}{\partial y^2} + Ge\frac{\partial \theta}{\partial x} = 0, \tag{36}$$

$$\frac{\partial \theta}{\partial t} + Pe\tilde{u}_{B\pm}\frac{\partial \theta}{\partial x} - Pe^2\frac{\partial \psi}{\partial x}\frac{d\tilde{T}_{B\pm}}{dy} = \frac{\partial^2\theta}{\partial x^2} + \frac{\partial^2\theta}{\partial y^2} + Pe\left(2\tilde{u}_{B\pm} - \tilde{\Gamma}_{\pm}\right)\frac{\partial \psi}{\partial y}. \tag{37}$$

The boundary conditions fulfilled by ψ and θ are easily inferred from Eqs. (14), (28) and (35), namely

$$y = 0, 1: \quad \psi = 0 = \frac{\partial \theta}{\partial y}. \tag{38}$$

Solutions of Eqs. (36)–(38) are sought in the form of plane waves,

$$\psi(x,y,t) = \Re\left\{\Psi(y)e^{\lambda t}e^{iax}\right\}, \quad \theta(x,y,t) = \Re\left\{\Theta(y)e^{\lambda t}e^{iax}\right\}, \tag{39}$$

where $\Re$ denotes the real part, the positive real constant a is the prescribed wave number, while $\lambda = \lambda_1 + i\lambda_2$ is a complex exponential growth rate. Its real part λ_1 influences the growth and decay of the perturbation, while its imaginary part λ_2 represents the frequency of the oscillations. Stability corresponds to $\lambda_1 < 0$, neutral stability corresponds to $\lambda_1 = 0$, while instability corresponds to $\lambda_1 > 0$.

By substituting Eq. (39) in Eqs. (36) and (37), one obtains

$$\Psi'' - a^2\Psi + iaGe\Theta = 0, \tag{40}$$

$$\Theta'' - \left(\lambda + iaPe\tilde{u}_{B\pm} + a^2\right)\Theta + Pe\left(2\tilde{u}_{B\pm} - \tilde{\Gamma}_{\pm}\right)\Psi' + iaPe^2\tilde{T}'_{B\pm}\Psi = 0, \tag{41}$$

where primes denote differentiation with respect to y. Elimination of Θ from Eqs. (40) and (41) yields a fourth order ordinary differential equation for $\Psi(y)$, namely

$$\begin{aligned} \Psi'''' - \left(\lambda + iaPe\tilde{u}_{B\pm} + 2a^2\right)\Psi'' - iaGePe\left(2\tilde{u}_{B\pm} - \tilde{\Gamma}_{\pm}\right)\Psi' \\ + a^2\left(\lambda + iaPe\tilde{u}_{B\pm} + a^2 + GePe^2\tilde{T}'_{B\pm}\right)\Psi = 0. \end{aligned} \tag{42}$$

The boundary conditions fulfilled by $\Psi(y)$ are easily deduced from Eqs. (38)–(40),

$$y = 0, 1: \quad \Psi = 0 = \Psi'' - a^2\Psi'. \tag{43}$$

Homogeneity of Eqs. (42) and (43) implies that $\Psi(y)$ is defined only up to an arbitrary overall scale factor. This feature leaves one the freedom to fix arbitrarily the value of $\Psi'(0)$. Then, one can set this quantity to 1, thus obtaining

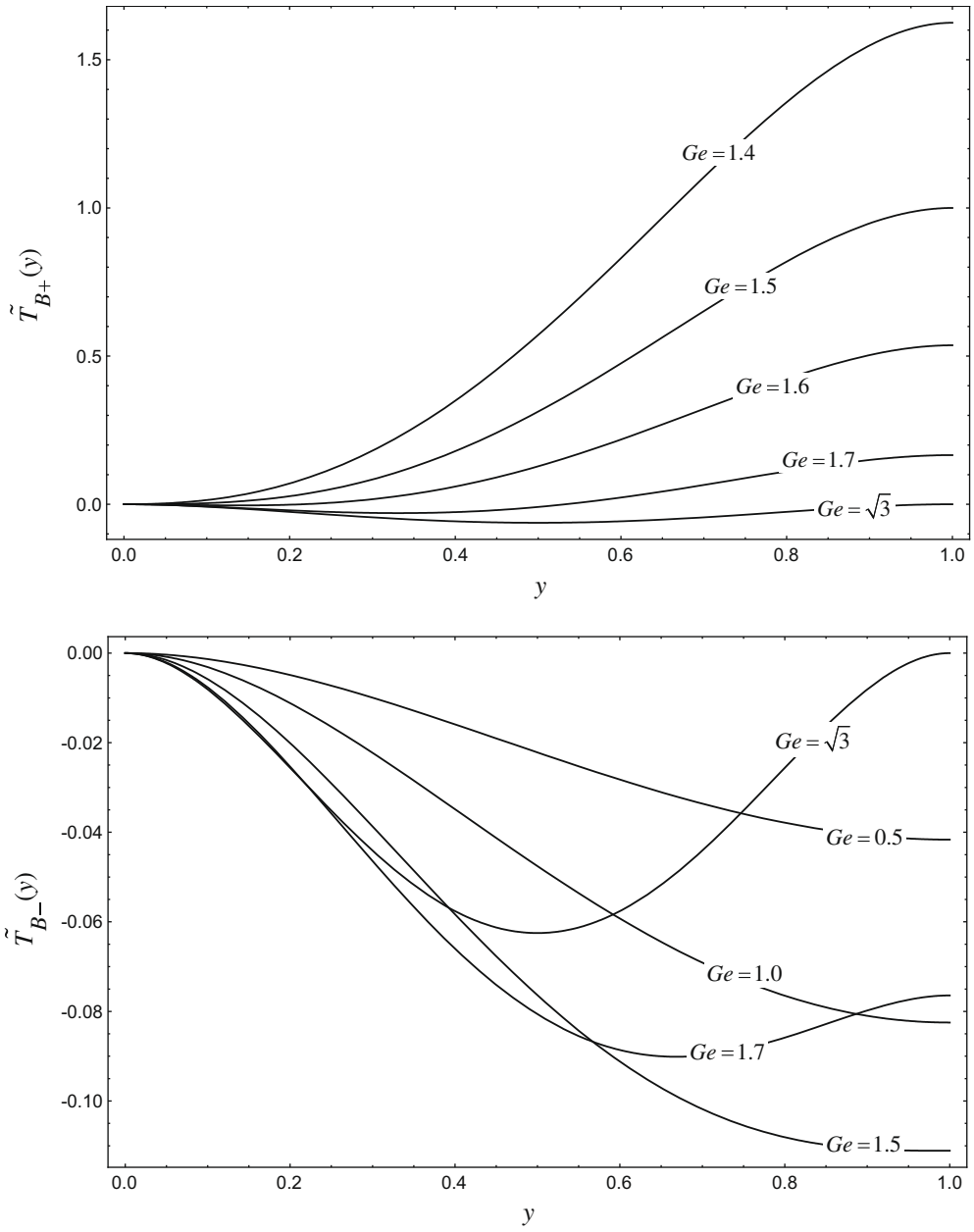

Fig. 2. Dual base-flow temperature profiles.

$$y = 0: \quad \Psi = 0, \quad \Psi' = 1, \quad \Psi''' = a^2, \tag{44}$$

$$y = 1: \quad \Psi = 0, \quad \Psi''' - a^2\Psi' = 0. \tag{45}$$

Eq. (42) can be rewritten as

$$\Psi'''' - \left[\lambda_1 + i\gamma + ia\frac{R}{Ge}(\tilde{u}_{B\pm} - 1) + 2a^2\right]\Psi'' - iaR\left(2\tilde{u}_{B\pm} - \tilde{\Gamma}_{\pm}\right)\Psi' + a^2\left[\lambda_1 + i\gamma + ia\frac{R}{Ge}(\tilde{u}_{B\pm} - 1) + a^2 + \frac{R^2}{Ge}\tilde{T}'_{B\pm}\right]\Psi = 0, \tag{46}$$

where

$$\gamma = \lambda_2 + aPe, \quad R = GePe. \tag{47}$$

Eqs. (44)–(46) represent an eigenvalue problem. One can set $\lambda_1 = 0$ in order to determine the neutral stability curve and fix the value of Ge. Then, for any wave number a, one can determine the eigenfunction Ψ and the corresponding eigenvalues (γ, R). By minimizing R with respect to a over the neutral stability curve, one can determine the critical values $(a_{cr}, \gamma_{cr}, R_{cr})$ corresponding to a given Ge. This analysis can be performed either with reference to the branch $\Gamma = \Gamma_-$ or to the branch $\Gamma = \Gamma_+$ of the dual base flow space. The computation can be performed by solving numerically Eq. (46) subject to the boundary conditions (44) and (45). Methods suitable for ODEs, such as the predictor–corrector Adams method and Runge–Kutta methods, can be easily implemented by using function `NDSolve` within the *Mathematica* (© Wolfram Research, Inc.) environment. The strategy to get the pairs (γ, R) on the neutral stability curve consists in a shooting technique based on the following steps:

- solve Eqs. (44) and (46) as an initial value problem, by complementing the conditions at $y = 0$ with the guessed value of $\Psi''(0)$;
- the boundary conditions at $y = 1$ are used as constraints to determine γ, R as well as to check the guessed value of $\Psi''(0)$.

Table 1
Critical values for the onset of transverse rolls corresponding to different *Ge*.

Ge	a_{cr}	R_{cr}	γ_{cr}
$\Gamma=\Gamma_-$			
$\to 0$	0	10.9545	0.000
10^{-8}	0	10.9545	0.000
10^{-6}	0	10.9545	0.000
10^{-5}	0	10.9545	0.000
10^{-4}	0	10.9545	0.000
10^{-3}	0	10.9545	0.000
10^{-2}	0	10.9545	0.000
10^{-1}	0	10.9619	0.000
0.5	0	11.1608	0.000
1	0	12.2031	0.000
1.2	0	13.4955	0.000
1.4	0	17.7709	0.000
1.45	2.5777	19.7540	−0.063
1.5	2.6404	20.1040	−1.06
1.6	2.7094	21.0747	−3.65
1.65	2.7231	21.9441	−5.78
1.7	2.7359	23.7905	−10.2
1.72	2.7746	25.6368	−15.0
1.732	2.9774	29.9106	−29.8
$\sqrt{3}$	2.9986	30.2983	−31.4
$\Gamma=\Gamma_+$			
1.65	5.5886	89.4901	−517.
1.7	3.9415	49.5949	−138.
1.72	3.4198	39.0036	−72.5
1.732	3.0203	30.7010	−33.0
$\sqrt{3}$	2.9986	30.2983	−31.4

The procedure is well posed, since the boundary conditions at $y=1$, Eq. (45) are four real equations, being Ψ a complex valued function. In fact, γ, R and $\Psi''(0)$ correspond to four real unknowns.

Table 1 contains critical values $(a_{cr},\gamma_{cr},R_{cr})$ corresponding to $Ge\leqslant\sqrt{3}$, for the branch $\Gamma=\Gamma_-$, and to $3/2<Ge\leqslant\sqrt{3}$, for the branch $\Gamma=\Gamma_+$. Interestingly enough, for $\Gamma=\Gamma_-$, one notices that (a_{cr},R_{cr}) are practically independent of *Ge* when $Ge\leqslant 10^{-2}$, while these values increase for a higher *Ge*. In particular, for sufficiently small values of *Ge*, function $R(a)$ on the neutral stability curve is monotonic increasing, so that $a_{cr}=0$. On the other hand, for large values of *Ge* and $\Gamma=\Gamma_-$, $R(a)$ on the neutral stability curve reaches the absolute minimum for a value $a_{cr}>0$ that increases with *Ge*. The values of (a_{cr},R_{cr}) referring to the branch $\Gamma=\Gamma_+$ rapidly increase as *Ge* decreases from its maximum value $Ge=\sqrt{3}$. Fig. 3 displays the neutral stability curve in the plane (a,R) for the branch $\Gamma=\Gamma_-$ in the small-*Ge* regime that, according to the above discussion, means approximately $Ge\leqslant 10^{-2}$. The evolution of the neutral stability curves for large *Ge* from a monotonic increasing behaviour of $R(a)$ to a non-monotonic behaviour is displayed in Fig. 4. This figure, referring to the branch $\Gamma=\Gamma_-$, justifies the above described transition from $a_{cr}=0$ to $a_{cr}\neq 0$, for sufficiently large *Ge*.

It must be pointed out that it is quite hard to conceive of practical cases either in the field of geophysics or in engineering applications not included in the range $Ge\leqslant 10^{-2}$. Therefore, it appears as interesting to consider, for a finite R, the limiting case of Eq. (46) for $\Gamma=\Gamma_-$ and $Ge\to 0$,

$$\Psi''''-\left[\lambda_1+i\gamma+ia\frac{R}{2}(1-2y)+2a^2\right]\Psi''-iaR\Psi' +a^2\left[\lambda_1+i\gamma+ia\frac{R}{2}(1-2y)+a^2-\frac{R^2}{2}(y-y^2)\right]\Psi=0, \qquad (48)$$

where use has been made of Eqs. (25)–(27).

The solution of Eqs. (44), (45) and (48) can be sought analytically by a series method as described in Appendix A. This series has a very rapid convergence. In all the cases considered, evaluation with 6 digits accuracy can be achieved by truncating the sum to the first 40 terms. In particular, in Table 1, the critical values $(a_{cr},\gamma_{cr},R_{cr})$ for the limiting case $Ge\to 0$ are obtained by the series solution. A complete agreement of the series solution results with those for cases with small *Ge* obtained numerically is evidenced in this table.

Fig. 5 displays the streamlines $\psi=$ constant and the isotherms $\theta=$ constant corresponding to $Ge=\sqrt{3}$ and to critical conditions $a=a_{cr}=2.9986$, $R=R_{cr}=30.2983$ and $\gamma=\gamma_{cr}=-31.4$. As a consequence of Eqs. (39) and (47), the transverse rolls travel along the *x*-axis with a speed

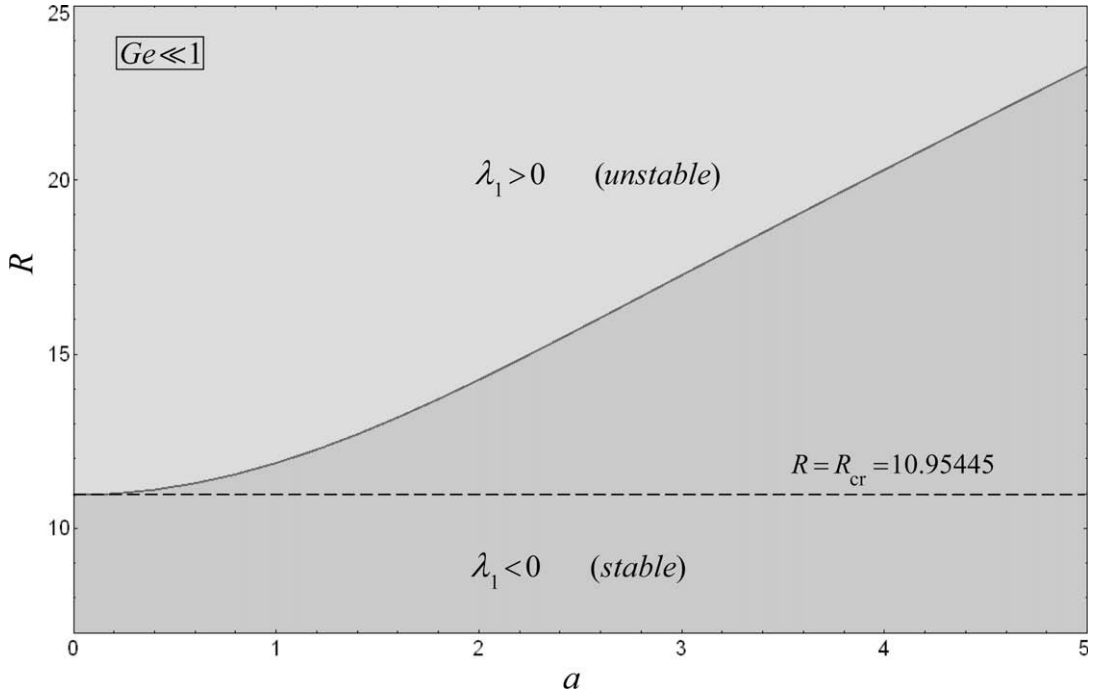

Fig. 3. Stability diagram for transverse rolls in the plane (a,R) (base flow branch $\Gamma=\Gamma_-$, in the limit of very small *Ge*).

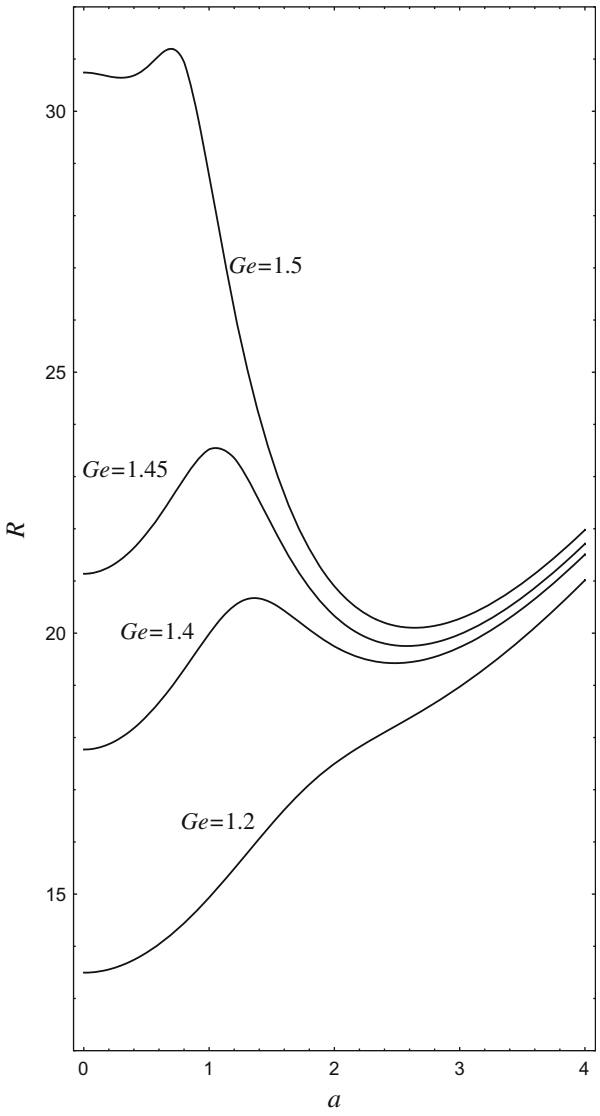

Fig. 4. Transverse rolls: neutral stability curves for very large values of Ge (base flow branch $\Gamma = \Gamma_-$).

$$c = -\frac{\lambda_2}{a} = Pe - \frac{\gamma}{a} = \frac{R}{Ge} - \frac{\gamma}{a}. \tag{49}$$

In the case illustrated in Fig. 5, one has $c = 27.949$.

4. Instability with respect to longitudinal rolls

Let us now consider disturbances for rolls which are parallel to the $\bar{x}$-direction, namely

$$U = 0, \quad V = V(y,z,t), \quad W = W(y,z,t), \quad \theta = \theta(y,z,t). \tag{50}$$

If one defines a streamfunction ψ, such that

$$V = -\frac{\partial \psi}{\partial z}, \quad W = \frac{\partial \psi}{\partial y}, \tag{51}$$

Eqs. (29), (31) and (32) are identically satisfied, while Eqs. (30) and (33) may be rewritten in the form

$$\frac{\partial^2 \psi}{\partial y^2} + \frac{\partial^2 \psi}{\partial z^2} + Ge\frac{\partial \theta}{\partial z} = 0, \tag{52}$$

$$\frac{\partial \theta}{\partial t} - Pe^2 \frac{\partial \psi}{\partial z}\frac{d\tilde{T}_{B\pm}}{dy} = \frac{\partial^2 \theta}{\partial y^2} + \frac{\partial^2 \theta}{\partial z^2}. \tag{53}$$

Moreover, ψ and θ fulfil the boundary conditions

$$y = 0, 1: \quad \psi = 0 = \frac{\partial \theta}{\partial y}. \tag{54}$$

As in the case of transverse rolls, solutions of Eqs. (52)–(54) are expressed as plane waves,

$$\psi(y,z,t) = \Re\left\{\Psi(y)e^{\lambda t}e^{iaz}\right\}, \quad \theta(y,z,t) = \Re\left\{\Theta(y)e^{\lambda t}e^{iaz}\right\}, \tag{55}$$

where the positive wave number a is prescribed, while $\lambda = \lambda_1 + i\lambda_2$ is the complex exponential growth rate. By substituting Eq. (55) in Eqs. (52) and (53), one obtains

$$\Psi'' - a^2\Psi + iaGe\Theta = 0, \tag{56}$$

$$\Theta'' - \left(\lambda + a^2\right)\Theta + iaPe^2\tilde{T}'_{B\pm}\Psi = 0. \tag{57}$$

Eqs. (56) and (57) lead to a fourth order ordinary differential equation for $\Psi(y)$, namely

$$\Psi'''' - \left(\lambda + 2a^2\right)\Psi'' + a^2\left(\lambda + a^2 + GePe^2\tilde{T}'_{B\pm}\right)\Psi = 0. \tag{58}$$

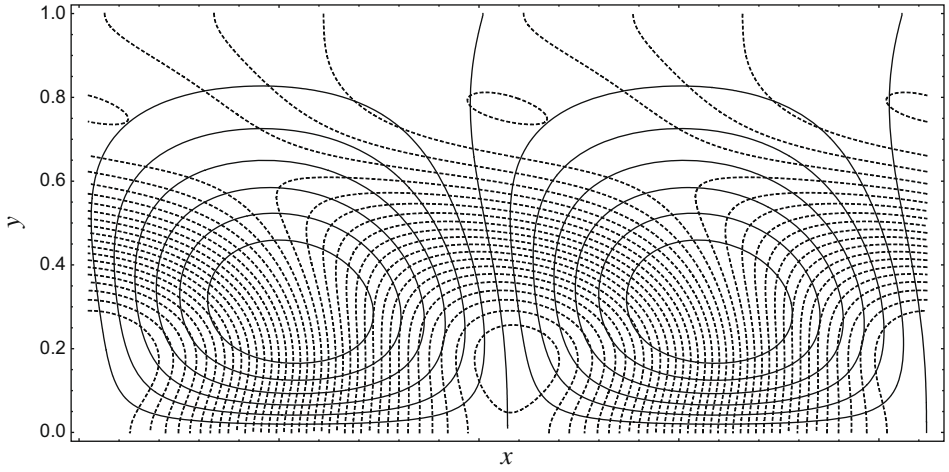

Fig. 5. Transverse rolls: streamlines ψ = constant (solid lines) and isotherms θ = constant (dashed lines) for $\lambda_1 = 0$, $Ge = \sqrt{3}$, $a = a_{cr} = 2.9986$, $R = R_{cr} = 30.2983$ and $\gamma = \gamma_{cr} = -31.4$.

When looking for the neutral stability condition, one can set $\lambda_1 = 0$. Unlike in the case of transverse rolls, by setting also $\lambda_2 = 0$, one may obtain $\Psi(y)$ as a real valued function for any pair (Ge, Pe). This feature implies that the propagation speed, $c = -\lambda_2/a$, is zero for longitudinal rolls. In fact, one has

$$\Psi'''' - 2a^2\Psi'' + a^2\left(a^2 + \frac{R^2}{Ge}\tilde{T}'_{B\pm}\right)\Psi = 0. \tag{59}$$

The boundary conditions fulfilled by $\Psi(y)$ are easily deduced from Eqs. (54)–(56), as well as from the freedom to fix arbitrarily the value of $\Psi'(0)$,

$$y = 0: \quad \Psi = 0, \quad \Psi' = 1, \quad \Psi''' = a^2, \tag{60}$$

$$y = 1: \quad \Psi = 0, \quad \Psi''' - a^2\Psi' = 0. \tag{61}$$

The procedure to solve Eqs. (59)–(61) as an eigenvalue problem is the same as adopted in the case of transverse rolls, even if one has in this case a simpler real ODE to deal with.

Table 2 contains critical values $(a_{cr}, \gamma_{cr}, R_{cr})$ corresponding to $Ge \leqslant \sqrt{3}$, for the branch $\Gamma = \Gamma_-$, and to $3/2 < Ge < \sqrt{3}$, for the branch $\Gamma = \Gamma_+$. Similarly to the case of transverse rolls (Table 1), for $\Gamma = \Gamma_-$, one notices that (a_{cr}, R_{cr}) are practically independent of Ge when $Ge \leqslant 10^{-1}$, while (a_{cr}, R_{cr}) increase for larger values of Ge. A comparison between Tables 1 and 2 reveals that the critical values of a and R are exactly the same for transverse rolls and for longitudinal rolls as far as Ge is sufficiently small, *i.e.* $Ge \leqslant 10^{-2}$. Another important result one can draw from Tables 1 and 2 is that longitudinal rolls instabilities occur for values of R equal or smaller than those needed for transverse rolls instabilities. In Tables 1 and 2, there is just one exception to this rule: the rather extreme case $Ge = 1.65$ for the branch $\Gamma = \Gamma_+$.

As in the analysis of transverse rolls, the limit $Ge \to 0$ for a finite R appears to be very significant also in the present case. In this limit, the fourth order ODE Eq. (59) is simplified to

$$\Psi'''' - 2a^2\Psi'' + a^2\left[a^2 - \frac{R^2}{2}(y - y^2)\right]\Psi = 0. \tag{62}$$

Table 2
Critical values for the onset of longitudinal rolls corresponding to different Ge.

Ge	a_{cr}	R_{cr}
$\Gamma = \Gamma_-$		
$\to 0$	0	10.9545
10^{-8}	0	10.9545
10^{-6}	0	10.9545
10^{-5}	0	10.9545
10^{-4}	0	10.9545
10^{-3}	0	10.9545
10^{-2}	0	10.9545
10^{-1}	0	10.9545
0.5	0	10.9570
1	0	11.0108
1.2	0	11.1012
1.4	0	11.3409
1.45	0	11.4568
1.5	0	11.6190
1.6	0	12.2403
1.65	0	12.9524
1.7	0	14.9136
1.72	0	17.8408
1.732	2.7118	25.7346
$\sqrt{3}$	2.8064	26.2711
$\Gamma = \Gamma_+$		
1.65	7.3087	90.1559
1.7	4.8147	48.0495
1.72	3.9353	36.6194
1.732	2.8957	26.8143
$\sqrt{3}$	2.8064	26.2711

The solution of Eq. (62) can be determined by a power series method as described in Appendix A.

The evolution of the neutral stability curves for large Ge from a monotonic increasing behaviour of $R(a)$ to a non-monotonic behaviour is shown in Fig. 6. This figure, referring to the branch $\Gamma = \Gamma_-$, justifies the transition from $a_{cr} = 0$ to $a_{cr} \neq 0$ displayed in Table 2, for Ge larger than 1.7.

Fig. 7 displays the streamlines $\psi =$ constant and the isotherms $\theta =$ constant corresponding to $Ge = \sqrt{3}$, *i.e.* the maximum allowed value of Ge, and to critical conditions $a = a_{cr} = 2.8064$ and $R = R_{cr} = 26.2711$.

With reference to the branch $\Gamma = \Gamma_-$, a comparison between the neutral stability curves in the limit $Ge \to 0$ for transverse rolls and for longitudinal rolls is given in Fig. 8. These curves have been determined by adopting the power series solutions found for very small Ge. As expected, this figure shows that instabilities to longitudinal rolls arise for smaller values of R than those needed for the onset of transverse rolls.

In Appendix B, we present a straightforward analytical procedure to show that the critical value of R for the branch $\Gamma = \Gamma_-$ in the small-Ge limit is in fact $R_{cr} = \sqrt{120} \cong 10.954451$, in agreement with the numerical results given in Tables 1 and 2, and Figs. 3 and 8.

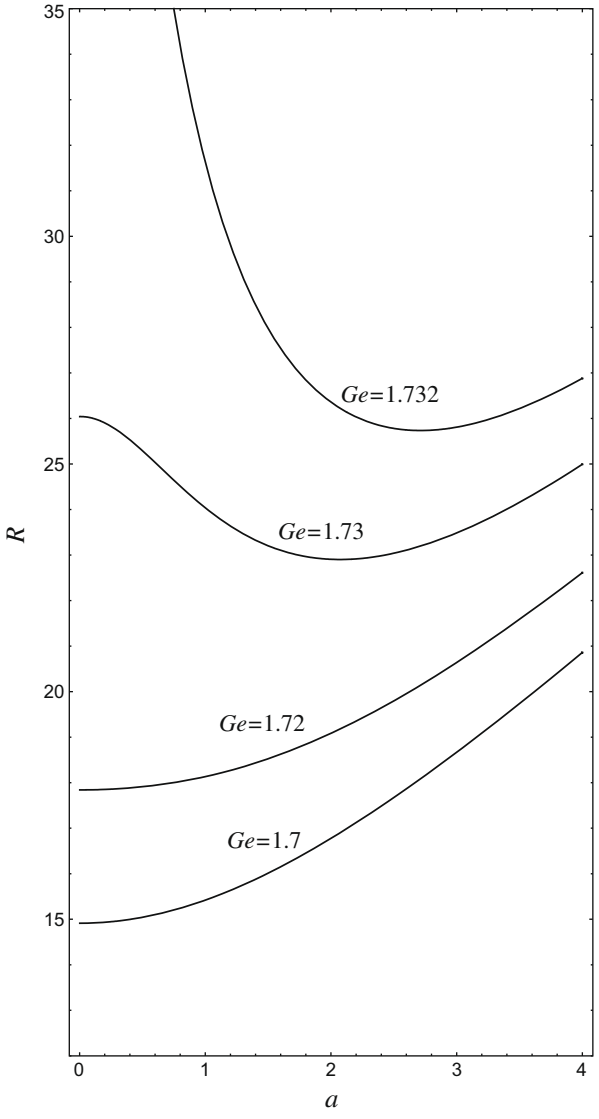

Fig. 6. Longitudinal rolls: neutral stability curves for very large values of Ge (base flow branch $\Gamma = \Gamma_-$).

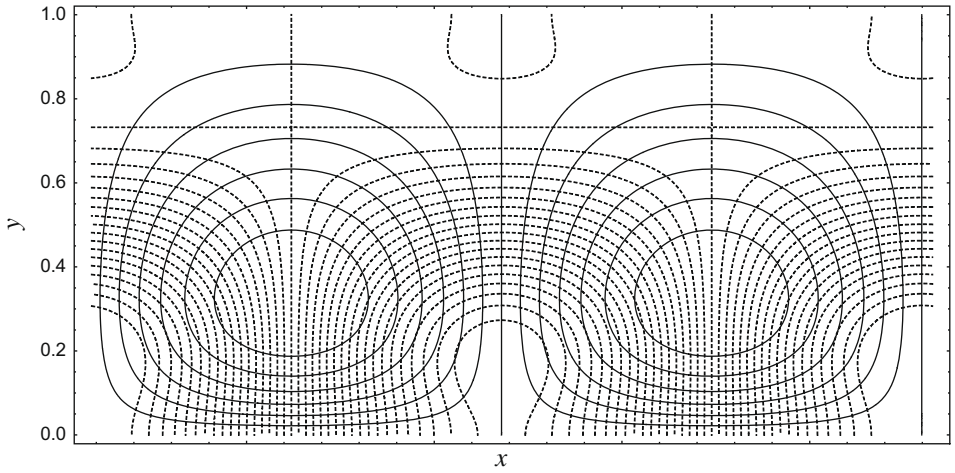

Fig. 7. Longitudinal rolls: streamlines $\psi = \text{constant}$ (solid lines) and isotherms $\theta = \text{constant}$ (dashed lines) for $\lambda_1 = 0$, $Ge = \sqrt{3}$, $a = a_{cr} = 2.8064$ and $R = R_{cr} = 26.2711$.

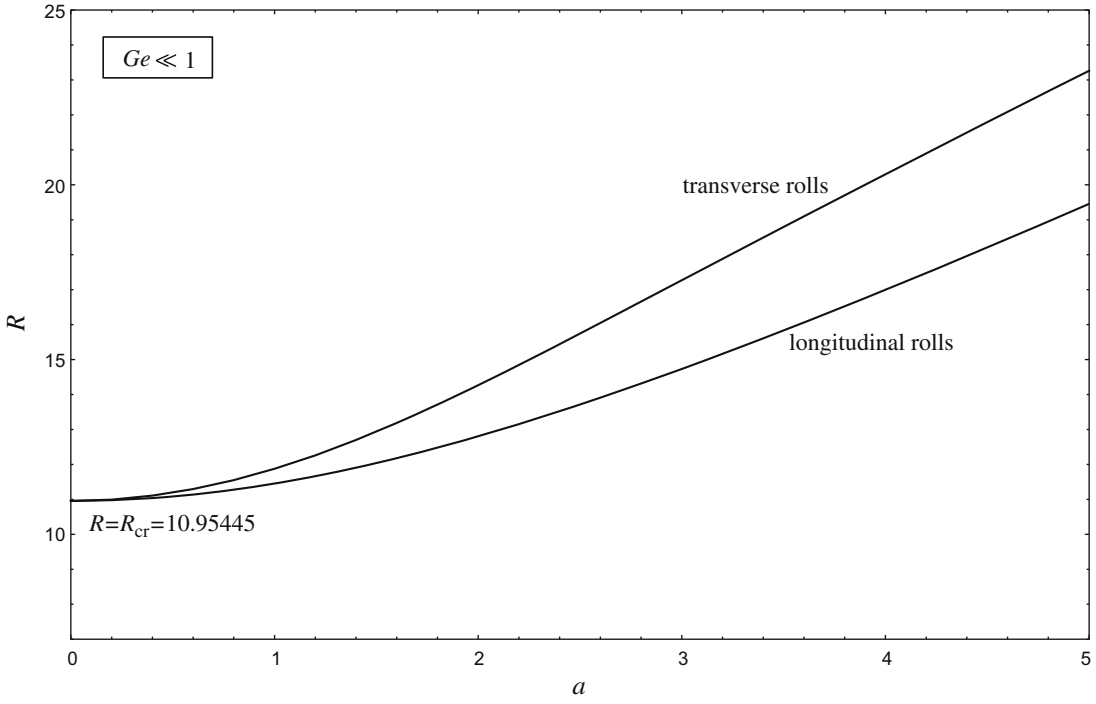

Fig. 8. Neutral stability curves for longitudinal rolls and for transverse rolls in the plane (a, R) (base flow branch $\Gamma = \Gamma_-$, in the limit $Ge \to 0$).

5. Concluding remarks

A linear stability analysis of buoyant flows with viscous dissipation in a horizontal porous layer has been performed. The walls have been considered as adiabatic and impermeable, so that the viscous heating of the system is the only cause of horizontal and vertical thermal gradients. The local balance equations have been written according to the Darcy–Boussinesq model. The non-dimensional formulation of the equations revealed that the system is governed by two parameters: the Gebhart number, *Ge*, and the Péclet number, *Pe*, associated to the basic mass flow rate in the layer.

It has been shown that, for every given pair of values $\{Ge, Pe\}$ such that $Ge \leqslant \sqrt{3}$, there exist two stationary parallel flow solutions (*dual flows*): the Γ_--solution and the Γ_+-solution. Both these solutions are characterised by a linear velocity profile and by a temperature distribution expressed as a fourth-order polynomial function of the vertical coordinate and as a linear function of the streamwise horizontal coordinate. The Γ_--solution can develop convective instabilities for every $Ge \leqslant \sqrt{3}$, while the Γ_+-solution can develop convective instabilities only for $3/2 < Ge \leqslant \sqrt{3}$.

The development of convective instabilities depends on the value of *Pe*: the larger is the value of *Pe* the greater is the effect of viscous dissipation and, as a consequence, the larger is the vertical temperature gradient inside the layer. The product $R = GePe$ has been defined as the order parameter for the transition from the stable to the unstable regime. The reason is that, in the physically important cases of very small *Ge*, the critical value of the parameter *R* becomes independent of *Ge*. Stated differently, for $Ge \ll 1$, the

critical value of Pe for the onset of convective instabilities is inversely proportional to Ge. Wavelike disturbances propagating in the basic flow direction (*transverse rolls*) become unstable for $Pe > Pe_{cr} = 10.9545/Ge$, when $Ge \leqslant 0.01$. The same expression of Pe_{cr} holds also for wavelike disturbances developing in the direction orthogonal to the basic flow (*longitudinal rolls*), as long as $Ge \leqslant 0.1$. Most practical cases hardly fall out of the domain $Ge \leqslant 0.01$, so that one may say that the onset of transverse and longitudinal rolls is associated with the same R_{cr}. Within this parametric domain, the neutral stability curves in the plane (a, R), referring either to transverse or to longitudinal rolls, are monotonic increasing so that the critical wavenumber a_{cr} is zero.

For the sake of completeness in the mathematical analysis of the present problem, also higher values of Ge have been investigated. It has been pointed out that, for values of Ge next to the maximum allowed threshold $\sqrt{3}$, both the Γ_--solution and the Γ_+-solution develop instabilities of the form of longitudinal and transverse rolls, corresponding to a nonvanishing a_{cr}. In almost all the cases examined, longitudinal rolls are the most unstable as they correspond to the smallest value of R_{cr}. In the case of the Γ_+-solution, the values of R_{cr} increase as Ge decreases from the maximum value $\sqrt{3}$ and are likely to tend to infinity as $Ge \to 3/2$. As stated above, no convective instabilities are developed by the Γ_+-solution for $Ge \leqslant 3/2$.

Adiabatic flows, *i.e.* flows in regions with adiabatic boundaries, are the kind of flows where viscous dissipation arises as the only cause of the non-uniform temperature distribution. As a consequence, the onset of convective instabilities can be immediately ascribed to the effect of viscous dissipation. The present analysis is mainly aimed to highlight this reasoning by an explicit analysis of a porous flow case. Physically, due to the very narrow size of the passages permitted to the fluid motion, porous flows and microchannel flows are conditions where viscous heating phenomena can be very important. An interesting opportunity for future research can be the extension of the present stability analysis to cases involving clear fluids.

Appendix A

A.1. Transverse rolls

Eqs. (44) and (48) can be solved by a power series method. Let us set $\lambda_1 = 0$ in order to study neutral stability. One can express $\Psi(y)$ as

$$\Psi(y) = \sum_{n=0}^{\infty} \frac{A_n}{n!} y^n. \tag{A1}$$

On account of Eq. (44), one easily obtains

$$A_0 = 0, \quad A_1 = 1, \quad A_2 = \eta + i\xi, \quad A_3 = a^2, \tag{A2}$$

where $\eta + i\xi$ is the guessed value of $\Psi''(0)$. Higher order coefficients A_n can be determined by substituting Eq. (A1) into Eq. (48) and collecting like powers of y. Then, one has

$$A_4 = \left[2a^2 + i\left(\gamma + a\frac{R}{2}\right)\right](\eta + i\xi) + iaR, \quad A_5 = a^4, \tag{A3}$$

and the recursive relation

$$\begin{aligned} A_{n+4} = &\left[2a^2 + i\left(\gamma + a\frac{R}{2}\right)\right]A_{n+2} - iaR(n-1)A_{n+1} \\ &- a^2\left[a^2 + i\left(\gamma + a\frac{R}{2}\right)\right]A_n + a^2\left(\frac{R^2}{2} + iaR\right)nA_{n-1} \\ &- \frac{1}{2}a^2R^2n(n-1)A_{n-2}, \quad \forall n \geqslant 2. \end{aligned} \tag{A4}$$

A.2. Longitudinal rolls

Eqs. (60) and (62) can be solved by a similar series method. Let us set $\lambda_1 = 0$ in order to study neutral stability, then one can express $\Psi(y)$ as in Eq. (A1). On account of Eq. (60), one obtains

$$A_0 = 0, \quad A_1 = 1, \quad A_2 = \eta, \quad A_3 = a^2, \tag{A5}$$

where η is the guessed value of $\Psi''(0)$. Coefficients A_n, for $n > 3$, can be determined by substituting Eq. (A1) into Eq. (62) and collecting like powers of y. Then, one has

$$A_4 = 2a^2\eta, \quad A_5 = a^4, \tag{A6}$$

and the recursive relation

$$A_{n+4} = 2a^2A_{n+2} - a^4A_n + \frac{1}{2}a^2R^2nA_{n-1} - \frac{1}{2}a^2R^2n(n-1)A_{n-2}, \quad \forall n \geqslant 2. \tag{A7}$$

Appendix B

Upon setting $\lambda = 0$, Eqs. (56) and (57) are

$$\Psi'' - a^2\Psi + iaGe\Theta = 0, \tag{B1}$$

$$\Theta'' - a^2\Theta + iaPe^2\tilde{T}'_{B\pm}\Psi = 0. \tag{B2}$$

The system may be simplified by setting $\Psi = iaGe\Phi$, and we get,

$$\Phi'' - a^2\Phi + \Theta = 0, \tag{B3}$$

$$\Theta'' - a^2\Theta - a^2Pe^2Ge\tilde{T}'_{B\pm}\Phi = 0, \tag{B4}$$

which is real. We are interested in determining the onset of convection in the small-a limit, and therefore we may expand solutions in a power series in a^2. Let

$$(\Phi, \Theta) = (\Phi_0, \Theta_0) + a^2(\Phi_2, \Theta_2) + \cdots \tag{B5}$$

At leading order the equations are

$$\Theta_0'' = 0, \quad \Phi_0'' + \Theta_0 = 0, \tag{B6}$$

for which the solutions are,

$$\Theta_0 = 1, \quad \Phi_0 = (y - y^2)/2. \tag{B7}$$

Here we have set Θ_0 to an arbitrary nonzero constant, which is permissible since this is a linear stability analysis. At $O(a^2)$, the equation for Θ_2 is,

$$\Theta_2'' = \Theta_0 + Pe^2Ge\tilde{T}'_{B\pm}\Phi_0. \tag{B8}$$

Given that

$$\int_0^1 \Theta_2''dy = 0, \tag{B9}$$

it follows that the similar integral of the right hand side of Eq. (B8) must also be zero. Hence we have the solvability condition,

$$\frac{1}{2}Pe^2Ge\int_0^1 (y - y^2)\tilde{T}'_{B\pm}(y)dy = -1. \tag{B10}$$

We are interested in the branch $\Gamma = \Gamma_-$ of the dual solutions, and in the small-Ge limit. Therefore we may use the solution for $\tilde{T}_{B-}(y)$ which is given in Eq. (26), namely that $\tilde{T}_{B-}(y) \sim y^2(2y - 3)Ge/12$ at leading order. Therefore Eq. (B10) yields,

$$\frac{Pe^2Ge^2}{120} = 1 \Rightarrow R = GePe = \sqrt{120} \cong 10.954451, \tag{B11}$$

which confirms the numerical results given in Tables 1 and 2, and Figs. 3 and 8.

References

[1] H.C. Brinkman, Heat effects in capillary flow I, Appl. Sci. Res. A 2 (1951) 120–124.
[2] G.P. Celata, G.L. Morini, V. Marconi, S.J. McPhail, G. Zummo, Using viscous heating to determine the friction factor in microchannels – an experimental validation, Exp. Therm. Fluid Sci. 30 (2006) 725–731.
[3] W.P. Breugem, D.A.S. Rees, A derivation of the volume-averaged Boussinesq equations for flow in porous media with viscous dissipation, Transport Porous Med. 63 (2006) 1–12.
[4] D.A. Nield, The modeling of viscous dissipation in a saturated porous medium, ASME J. Heat Transfer 129 (2007) 1459–1463.
[5] A. Barletta, Laminar mixed convection with viscous dissipation in a vertical channel, Int. J. Heat Mass Transfer 41 (1998) 3501–3513.
[6] E.W. Mureithi, D.P. Mason, On the stability of a forced-free boundary layer flow with viscous heating, Fluid Dyn. Res. 31 (2002) 65–78.
[7] E. Magyari, B. Keller, Buoyancy sustained by viscous dissipation, Transport Porous Med. 53 (2003) 105–115.
[8] A. Pantokratoras, Effect of viscous dissipation in natural convection along a heated vertical plate, Appl. Math. Model. 29 (2005) 553–564.
[9] R.B. Mansour, N. Galanis, C.T. Nguyen, Dissipation and entropy generation in fully developed forced and mixed laminar convection, Int. J. Therm. Sci. 45 (2006) 998–1007.
[10] A. Barletta, E. Magyari, B. Keller, Dual mixed convection flows in a vertical channel, Int. J. Heat Mass Transfer 48 (2005) 4835–4845.
[11] A. Barletta, E. Magyari, I. Pop, L. Storesletten, Mixed convection with viscous dissipation in a vertical channel filled with a porous medium, Acta Mech. 194 (2007) 123–140.
[12] D.A. Nield, A. Bejan, Convection in Porous Media, third ed., Springer, New York, 2006.
[13] D.A.S. Rees, Stability of Darcy–Bénard convection, in: K. Vafai (Ed.), Handbook of Porous Media, Begell House, 2000, pp. 521–558.
[14] P.A. Tyvand, Onset of Rayleigh–Bénard convection in porous bodies, in: D.B. Ingham, I. Pop (Eds.), Transport Phenomena in Porous Media II, Elsevier, 2002, pp. 82–112.
[15] C.W. Horton, F.T. Rogers Jr., Convection currents in a porous medium, J. Appl. Phys. 16 (1945) 367–370.
[16] E.R. Lapwood, Convection of a fluid in a porous medium, Proc. Camb. Philos. Soc. 44 (1948) 508–521.
[17] M. Prats, The effect of horizontal fluid flow on thermally induced convection currents in porous mediums, J. Geophys. Res. 71 (1966) 4835–4838.
[18] X.S. He, J.G. Georgiadis, Natural convection in porous media: effect of weak dispersion on bifurcation, J. Fluid Mech. 216 (1990) 285–298.
[19] D.A.S. Rees, The effect of inertia on the onset of mixed convection in a porous layer heated from below, Int. Commun. Heat Mass Transfer 24 (1997) 277–283.
[20] D.A.S. Rees, E. Magyari, B. Keller, Vortex instability of the asymptotic dissipation profile in a porous medium, Transport Porous Med. 61 (2005) 1–14.
[21] A. Barletta, M. Celli, D.A.S. Rees, The onset of convection in a porous layer induced by viscous dissipation: A linear stability analysis, Int. J. Heat Mass Transfer 52 (2009) 337–344.